Final Technical Report

Grant or Contract Number: ONR N00014-19-1-2480
Date Prepared: 11/28/2022
Project Title: The Wesleyan University Research Effort for: Waveform Shaping Protocols for Targeted Electromagnetic Attacks
Performing Period: 07/01/2019-10/31/2022
Program Manager: Mr. Peter A. Morrison (ONR CODE-35)
Principle Investigator: Tsampikos Kottos, (860)-685-2036, tkottos@wesleyan.edu
Wesleyan University

Prepared by : Tsampikos Kottos
Department of Physics, Wesleyan University
Exley Science Tower, 265 Church Street
Middletown CT-06459, USA
Tel: 860-6852036
Email: tkottos@wesleyan.edu

This work was sponsored by the Office of Naval Research (ONR), under grant (or contract) number N00014-19-1-2480. The views and conclusions contained herein are those of the authors only and should not be interpreted as representing those of ONR, the U.S. Navy or the U.S. Government.

Project Summary

1. Rationale of Project, Objectives and Executive Summary of Basic Results

Abstract: The prospect of utilizing electromagnetic radiation to efficiently target and destroy sensitive electronic circuitry has been intensely pursued during the last years leading to a new class of weapons – directed energy weapons (DEWs). DEWs are highly advantageous since they allow for non-lethal attacks at the speed of light, precise targeting, rapid engagement of multiple targets, adjustable damage capacity, and low operational cost. In typical circumstances, the targets are inside complex enclosures (e.g., computer box, reverberation chamber, aircraft fuselage) resulting in wave scattering processes which are extremely sensitive to the exact geometry of the enclosure, the operating frequency, etc. Therefore, any effort to realize wavefronts with 100% targeting efficiency is meaningless. Even more challenging are the scenarios where the targeted electronics involve nonlinear elements (e.g., diodes). This project develops tools for the design of Waveforms with Enhanced TArgeting Capabilities (**WETAC**) of linear and nonlinear electronic targets that are located inside a complicated enclosure. On the counter-side, the effort also develops novel protection schemes against agile wavefronts that aim to damage sensitive US assets (e.g., radars).

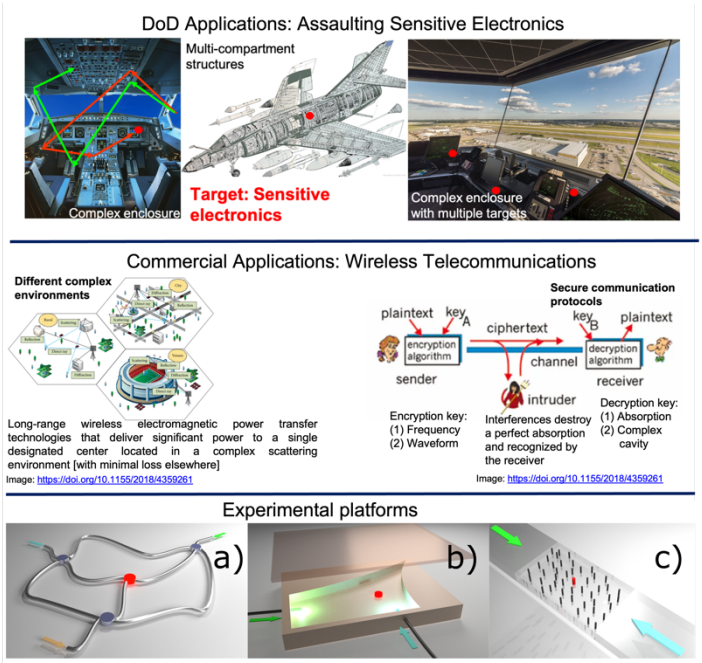

Figure 1:(Up) Potential scenarios where WETAC protocols can be useful in the framework of DEWs program; (Middle) Potential commercial applications of WETAC protocols; (Down) Theoretical/experimental settings where the efficiency of the WETAC protocols can be tested.

Objective: The proposed research has developed novel, effective means to direct energy onto sensitive linear or nonlinear electronic targets located inside a complex scattering environment. A parallel objective was the development of statistical theories (and its experimental implementation) that aim to design electromagnetic wavefronts with enhanced probability to assault sensitive electronic circuit elements located inside complex enclosures. These algorithms have utilized the universal statistical features of the scattering matrix describing such complex settings – supplemented by available intelligence of non-universal features. An overview of the DEW-scenarios, commercial applications, and theoretical/experimental settings where WETACs could be implemented are shown in Fig. 1. Finally, a parallel effort has been devoted to the development of counter-WETAC schemes, appropriate for the protection of sensitive electronic assets. A prominent example is a reflective photonic limiter i.e., a high-power filter that reflects to space harmful high-power radiation while it allows a low power radiation to go through.

Introduction: Lately, the idea of judiciously preparing agile wavefronts that upset sensitive electronics embedded in complex enclosures has been suggested as a new DEW paradigm. This approach makes use of notions based on time-reversal (TR) symmetry and it involves a two-step process. In the first step, the source/target emits a short pulse. After propagation, the time dependence of the waveform is recorded by an array of transducers, the so-called Time-Reversal Mirror (TRM). In the second step, these signals are reversed in time (wavefront shaping) and are re-emitted by the TRM. Due to the reversibility of the wave-equation, the time-reversed field back-propagates through the medium towards the position where the initial source/target is located — thus damaging the sensitive electronics. Disregarding subtle details, it was shown that the focusing of the back-propagating signal at the source position can be more efficient in the case of a non-homogenous medium or in the case of a complex (chaotic) enclosure. A somewhat different wavefront shaping scheme has also been developed in the optical domain and led to light focusing through strongly inhomogeneous media. The optics approach relies on self-learning protocols which exploit the existence of so-called open eigen-channels i.e., specific pathways within the disorder medium that allow for efficient wave propagation towards a specified focal point. It is important to stress that any small procedural error or alteration of the enclosure might be detrimental due to the complex interference effects underlying the scattering process in a chaotic enclosure. Thus, the design of a wavefront associated with a specific enclosure configuration is unfortunately irrelevant for the purposes of DEWs. The situation becomes more challenging when non-linear mechanisms are involved. In this case, the superposition principle over which the previous scattering matrix protocols rely breaks down, enforcing the necessity to develop altogether new theoretical schemes for wavefront focusing.

Background: The mesoscopic fluctuations of wave scattering in complex enclosures led to the development of so-called statistical electrodynamics. Within this framework, researchers have developed a statistical description of electromagnetic interferences (EMI) at any position inside a complex enclosure. This approach provides statistical tools that explain and analyze the sensitivity of the EMI in variations/replicas of the enclosure (subject to mesoscopic fluctuations). However, the current theory does not take into account the presence of non-linear elements (e.g. diodes) and their effect in the scattering process. The objective of the proposed research is (a) to develop theoretical tools for the (statistical) design of WETACs of electronic targets that are located inside complex enclosures; (b) experimentally demonstrate the efficiency of these algorithms; (c) incorporate the effects of nonlinear elements in the description of the scattering process from complex enclosures. Along these lines, we have also developed a description of the modal power distribution in nonlinear multimode photonic networks, using statistical mechanics principles coupled to spectral engineering techniques. Finally, the effort develops protective schemes of sensitive US assets from high-power/fluence incident radiation. This activity led to the realization of a novel reflective photonic limiter operating in the mm-wave range and to the development of a new concept of non-resonant reflective photonic limiter based on dynamical symmetries.

2. Highlights of Research Accomplishments

This grant supported (in total or partially) fifteen publications in peer review journals, two submitted papers, two patent applications (one approved and another awaiting approval), one PhD Thesis, and one undergraduate Honor Thesis. Four graduate students and eight undergraduate students have been involved in various aspects of the research effort. Below we provide some highlights of the research accomplishments associated with this effort.

I. Perfect Absorption in Complex Cavities with or Without Hidden Symmetries: We have proposed and investigated (collaboration with Prof. S. Anlage; UMD) the realization of coherent perfect absorption (CPA) wavefront protocols in case of absorbing targets (e.g. a receiving antenna) that are located inside a complex scattering system that does not have any geometric or dynamical (e.g. time-reversal) symmetries. CPA relies on wave interference effects that entrap the incident radiation inside a weakly lossy cavity/network, leading to its complete absorption. We implemented this scheme using first a fully connected microwave network constructed from coaxial cables connected by Tee-junctions, see Fig. 2a. By adding an electronically tuned lossy attenuator, we have continuously and precisely controlled the CPA condition. This has been achieved by identifying the CPA frequencies ω_{CPA} as the (complex) zeros of the measured scattering matrix which cross the real frequency axis as the variable attenuator is slowly tuned towards a critical loss γ_{CPA}. Under these conditions we have predicted and demonstrated perfect absorption in this complex scattering setting. Most importantly, our analysis allowed us to demonstrate that the concept of CPA can be extended beyond the case where time-reversal (TR) symmetry holds, greatly expanding the impact and utility of the CPA phenomenon. The TR violation has been achieved by introducing a circulator into the microwave graph, see Fig. 2a. To gain further confidence on the efficiency of the CPA protocol, we have also confirmed its viability in a two-dimensional quarter bow-tie chaotic billiard (see Fig. 2b).

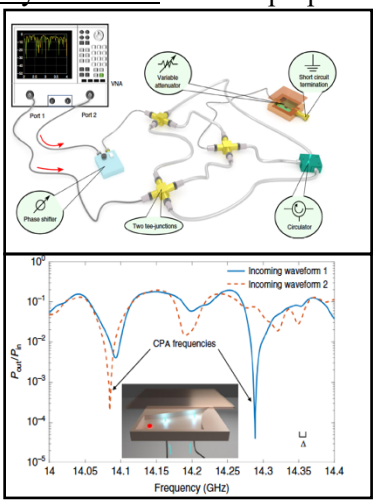

Figure 2: *(a)* The network set-up where the CPA schemes have been implemented. *(b)* A quarter bow-tie billiard (see inset) has been also used to test the CPA protocols. The red dot on the bow-tie represents the location of a point-like variable loss in the cavity. By injecting two different CPA waveforms (red and blue lines), the measured ratios of output power P_{out} to input power P_{in} as a function of the microwave frequency are plotted together. The scale bar of the mean mode spacing Δ is shown in the plot as well.

The CPA wavefront has been found by analyzing the M-dimensional scattering matrix $S(k;\gamma)$ (M are the number of scattering channels used to interrogate the cavity). The latter connects incoming $|I\rangle$ and outgoing $|O\rangle$ wave amplitudes i.e. $|O\rangle = S(k;\gamma)\,|I\rangle$ of a monochromatic wave with wavevector k (and frequency ω) which propagates via M-channels towards a lossy-target with loss-strength γ (which can be interpreted as the electrical conductivity of the target) and it is located inside a cavity. The components of the eigenvector $|\alpha_{CPA}(k_{CPA};\gamma_{CPA})\rangle = |I_{CPA}\rangle$ of the scattering matrix $S(k_{CPA};\gamma)$ that corresponds to a zero eigenvalue, $\lambda_S(k_{CPA};\gamma_{CPA}) = 0$, provide the linear combination (at each channel) of incident waves with frequency ω_{CPA} (and wavevector k_{CPA}) for which the outgoing waves are zero, i.e. $|O_{CPA}\rangle = S(k_{CPA};\gamma_{CPA})|I_{CPA}\rangle = 0$. The condition that the incident signal must be a propagating wave, imposes the additional requirement that k_{CPA} andω_{CPA} (for which $\lambda_S(k_{CPA};\gamma_{CPA}) = 0$), are real. Consequently, the CPA waveforms are identified with the real zeroes of the scattering matrix. It turns out that the CPA condition for a zero eigenvalue of the S-matrix is equivalent to a condition that the eigenvalue $0 \le \alpha(k,\gamma) \le 1$ of the absorption operator $A(k,\gamma) \equiv 1 - S^{+}(k;\gamma)S(k;\gamma)$ is unity i.e $\alpha(k_{CPA},\gamma_{CPA}) = 1$(complete absorption). Contrary, eigenvalues $\alpha(k,\gamma) = 0$ indicate that the incident energy is not absorbed. In Fig. 5b we demonstrate the success of our approach in identifying a CPA wavefront by analyzing the ratio $\Theta(\omega) \equiv \frac{output\ power}{input\ power} = \frac{P_{out}(\omega)}{P_{in}(\omega)}$ for a chaotic cavity. A vanishing $\Theta(\omega)$ (corresponding to unity absorbance A) indicates that the incident signal is completely absorbed by the targeted attenuator.

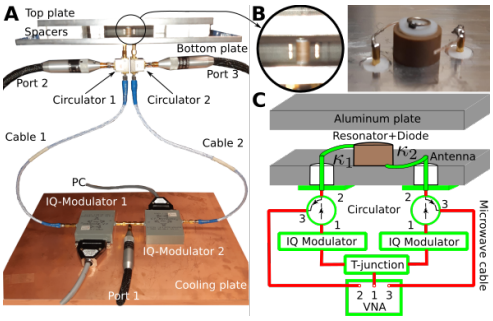

Figure 3: The experimental setup for NLCPA. a) Photograph of the experimental system including the connections. b) Zoom showing the experimental non-linear system consisting of a cylindrical dielectric resonator where a short-circuited diode is fixed above via a 1mm high Teflon spacer with the two transmitting/receiving antennas. c) Sketch detailing the setup.

II. Perfect Absorption wavefronts in case of Nonlinear Cavities: Waveform shaping (WFS) schemes for efficient energy deposition in weakly lossy targets is an ongoing challenge for many classical wave technologies relevant to wireless telecommunications, electro- magnetic warfare (e.g. for assault of sensitive electronics), etc. In many circumstances these targets are parts of a circuit, whose complex interconnectivity and/or the presence of non-linear elements challenges the viability of existing delicate WFS protocols like the CPA—see previous paragraph. Surprisingly, most of the CPA implementations have been performed under the assumption of scale invariance, i.e., the underlying wave systems were linear. The reasons for this lack of effort to identify nonlinear CPA (NLCPA) protocols is two-fold: From the theoretical side, one needs to develop new computational schemes which allow us to control, not only the relative phases and amplitudes of the incident waves, but also their absolute magnitude. From the experimental side, one might question the viability of such protocols due to nonlinearity-driven phenomena which might destroy the delicate interferences between various propagating waves or result in modulation instabilities making the NLCPA concept unrealistic. In collaboration with the experimental group of Prof. U. Kuhl (CNRS, France) we have developed and demonstrated the success of a NLCPA scheme using a simple microwave platform.

The experimental set-up is shown in Fig. 3 and consists of a dielectric resonator coupled to a short-circuited nonlinear lossy element (diode) sandwiched between two aluminum plates. This hybrid system demonstrates a non-linear response. The resonator is interrogated via two kink antennas curved around it. The antennas excite the first TE-resonance mode of the resonator (around 6.7 GHz), where the magnetic field $\vec{B}$ has only a z-component and the electric field lies parallel to the aluminum plates. The magnetic field couples to the short-circuited nonlinear diode thus inducing a non-linear behavior of the system. The incident and reflected waves of the system are separated by circulators connected to the source cable, the antenna, and the measuring port of the vector network analyzer (VNA). The excitation, with power P_{VNA}, is injected from port 1 of the VNA and it is splitted equally by a T-junction going through the IQ-modulators into the circulators. The IQ-modulators allow to vary the power and phase difference between the excitation lines. Thus, the measured complex transmission amplitudes S_{21}, S_{31} from port 1 to port 2 and to port 3 of the VNA give access to

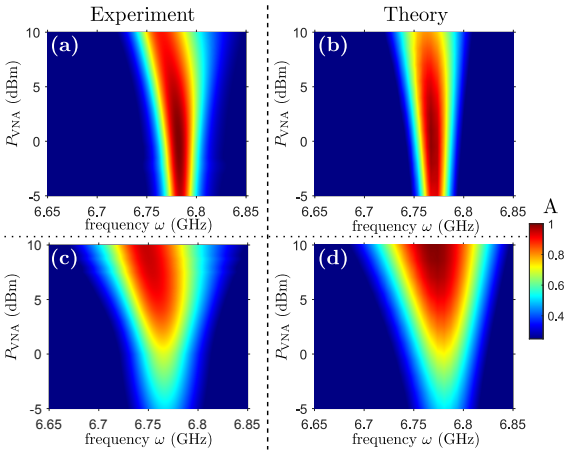

Figure 4: Absorbance A as a function of frequency ω and the injected power P_{VNA}. Left column shows our measurements, and the right column shows the results of our modeling. (Top row) The two antennas are weakly coupled. (Bottom row) The two antennas are moderately coupled.

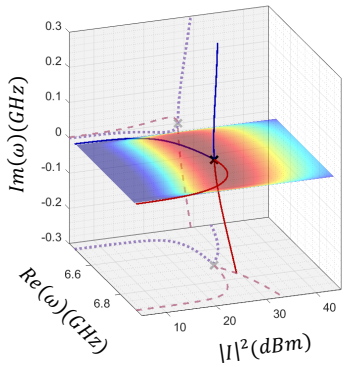

Figure 5: Trajectories (red and blue solid lines) of the complex zero frequencies ω of the outgoing fields as a function of input power. The dashed and dotted lines are projections of these trajectories on the corresponding plane. The absorbance A is reported as a density plot versus the frequency ω and the power P_{VNA} injected by the VNA. The interrogating antennas are perfectly coupled with the target.

the reflected power of the system $R = |S_{21}|^2 + |S_{31}|^2$. The total absorbance is then given by $A = 1 - R$.

In our analysis we have modeled the system using a coupled mode theory (CMT) and implemented a backward map approach to the scattering. By enforcing incoming boundary conditions, we have identified the NLCPA frequencies for which the system will be absorbing completely the incident radiation. These frequencies ω_{NLCPA} are the *real zeros* of the total reflected power i.e. $R(\omega_{NLCPA}) = 0$. In Fig. 4 (left column) we report the measured absorbance $A = 1 - \Theta(\omega)$ as a function of frequency ω and incident power P_{VNA}. The response function $\Theta(\omega)$ is defined as $\Theta(\omega) = \frac{output\ power}{input\ power} = \frac{P_{out}}{P_{in}}$. At the same figure (right column) we report the theoretical predictions associated with the parameters of the experiment.

The situation is more challenging when we consider perfect coupling between the antennas and the scatterer. In this case, we have found two complex roots within the propagating band, see Fig. 5. One of them (red trajectory) approaches the real plane from above, while the other one (blue trajectory) crosses the real plane from below as the intensity $|I|^2$ of the incident wave increases. At the crossing point (marked with a black cross) the two roots degenerate following a square-root cusp, and forming a new type of *self-induced exceptional point (EP) degeneracy* of CPAs. Since the EP occurs at the real ω −plane it constitutes a physically allowable CPA with absorbance $A = 1$. The latter, together with the fact that the two coalescing complex ω_{NLCPA} ``trajectories" have small imaginary part (see dashed lines projected in the imaginary ω −plane), results to the appearance of a (near-) perfect (i.e. $A = 99.99\%$) absorption for a broad frequency range. We stress that the broad-band absorption is counter-intuitive and challenges the CPA concept as a resonant phenomenon (see Fig. 2b).

This study involved a simple nonlinear lossy scatterer, thus ignoring the more complex cases where mesoscopic fluctuations (due to the complexity of the enclosure) are present. We have extended this study in order to consider cases where the lossy target is embedded inside a chaotic cavity. The algorithmic scheme that identifies the required amplitudes and relative phases of the injected NLCPA wavefronts has been developed using a Random Matrix Theory modeling that describes the complex cavity. Our analysis employed a non-linear coupled-mode theory that has been developed for the analysis of nonlinear wave-chaotic scattering (see next section), together with the CPA condition of zero outgoing waves

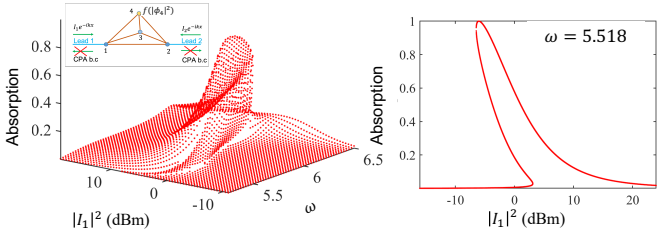

Figure 6: (Left) Absorption versus frequency and incident power of injected wavefront (keeping fixed the injected power from lead 2). In the inset we show a schematics of the NLCPA scenario (see also Figs. 7a-c). The nonlinear element is located at node 4 and it is described by a function that depends on the local value of the field. (Right) A cross-section of the previous plot at NLCPA frequency. The NLCPA wavefront leads to complete absorption and results in a bistability point for the absorbance.

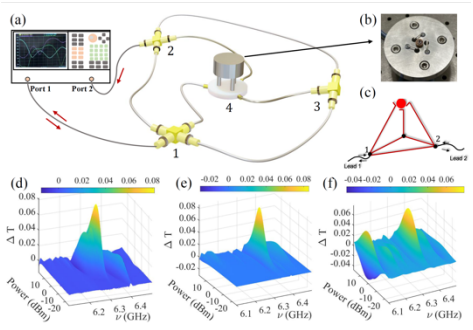

Figure 7: (a) The microwave tetrahedron graph with one nonlinear element at one of the vertices. The cables are connected by T or double T-junctions at each of the vertices 1,2,3 (marked as yellow) and (b) by kink antennas to a cylindrical dielectric scatterer that it is inductively coupled to a ring antenna which is short-circuited with a nonlinear diode. (c) Schematics of the tetrahedron graph scattering scenario; (d)-(f) The transmission difference for a left and right incident wave (of same amplitude and frequency) as a function of frequency and input power. (d) Experimental data; (e) simulations; (f) modeling.

which must be solved in a self-consistent manner to extract the incident frequency, amplitudes, and phases of the injected NLCPA wavefront. The algorithm has been tested for identifying the NLCPA wavefront in case of a metric graph with a (saturable) nonlinear element at one of the vertices. The numerical analysis confirmed the efficiency of the algorithm in identifying NLCPA wavefronts. We have shown the formation of strong absorption bistability effects with respect to input power (Fig. 6). The Wesleyan team is currently implementing this scheme in realistic targets using the platform of Fig. 7a-c.

III. Statistical Description of Scattering from Complex Enclosures with Discrete Nonlinear Elements: We have developed a nonlinear statistical electrodynamic formalism that accounts for the interplay between nonlinearities and wave-chaotic scattering. We have also developed an experimental platform which allowed us to test the validity of these theoretical predictions. The platform operates in the microwave regime and consists of a complex network of coaxial cables where one of the nodes is coupled to a diode (Figs. 7a-c). The motivation for choosing this platform was threefold: (a) networks of coaxial cables have been established as a testbed where both Random Matrix Theory (RMT) and semiclassical tools can be deployed with equal success in describing chaotic transport; (b) they have proven adequate model in describing electromagnetic transport in multi-compartment systems; (c) they are experimentally accessible in various wavelengths.

We have investigated the phenomenon of nonlinearity-induced asymmetric transport (Figs. 7d-f) and its statistics. We found an intimate relation between asymmetric transport (AT) in nonlinear wave-chaotic system and the structural asymmetry factor (SAF) that is determined by the geometric complexity of the underlying linear structure (Fig. 8). Our analysis showed that the SAF is equal to the asymmetric intensity range (AIR) defined as the range of input powers injected from opposite directions that lead to asymmetric transport. In case of lossless structures, the upper bound of the maximum transmission asymmetry $\Delta T_{max} \equiv T_{max} - T_{min} \leq T_{max}$ is a simple universal function of SAF (Fig. 8a). We concluded that AIR and maximum transmittance asymmetry vary disproportional to one another as SAF changes. Specifically, for small SAF, the AIR is small while the maximum transmission asymmetry is large and vise-versa (Fig.8a). A central result of our study was the identification of a class of lossy non-linear chaotic scattering settings whose transmission asymmetry bound exceeds the one of the corresponding lossless analogues (Fig. 8b). This typically occurs when losses are localized on the bonds or at a vertex that does not coincides to any of the vertices that are used to attach the leads or the nonlinear element. In this case a more complicated expression for the maximum transmittance asymmetry applies (Fig. 8b). We demonstrated experimentally that this class, does enhances the AIR while it does not degrade the transmission asymmetry (Fig. 8c). Finally, we established a novel RMT modeling that considers the interplay of nonlinearities and wave chaos and provides a description of the distribution of the transmission asymmetries ΔT. We have found that this distribution is determined by the intensity of the incident

field (Fig. 8d). Our nonlinear statistical theory allowed us also to evaluate the distribution of field intensities inside the chaotic cavity and specifically at the position of the nonlinear element (diode).

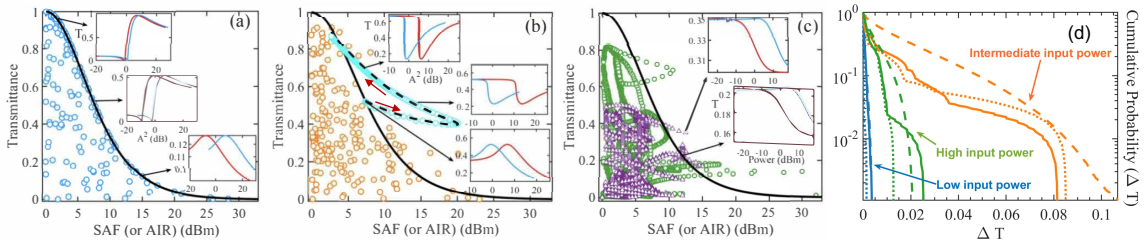

Figure 8: (a-c) Transmittance versus structural asymmetric factor (SAF) or asymmetric intensity range (AIR) for the graph of Fig. 7a. The black solid and dashed lines are theoretical predictions while the colored circles are simulations occurring at various wavelengths and graph configurations. (a) Lossless graph. The insets show the transmission versus input intensity from each of the two leads (marked as red and blue lines) for three different SAF graph configurations. (b) Lossy graph with losses imposed on node 3. The light blue circles indicate maximum transmittance for one graph configuration with increasing loss on node 3. The insets correspond to different losses for a fixed graph configuration. (c) Measurements (purple triangles) and simulations (green circles) for a graph with bond-losses and a lossy saturable nonlinearity. The insets show measurements corresponding to the same SAF but different maximum transmission values. (d) The cumulative probability distribution of transmission difference. A saturable nonlinearity is used. The blue, orange and green solid lines indicate measurements with input power -25, 1, 17 dBm respectively. The dotted lines are simulations with the same input power as in the experiment. The dashed lines are the RMT results.

IV. Statistical Description of Modal Power Distribution in Nonlinear Multimode Photonic Networks: The development of prognostic tools that predict the modal power distribution (MPD) of light in a photonic nonlinear multimode setting has important ramifications in the design of new platforms of high-power light sources. Typically, these predictive tools involve brute-force computations – a formidable process involving a mode-by-mode analysis of light propagation. Instead, in our recent studies we developed an alternative approach based on the implementation of statistical thermodynamics methods in nonlinear photonics. Leveraging on these statistical tools, we have developed a formalism that given (i) the resonant spectrum of a multimode photonic system; (ii) the total number of modes; (iii) the internal energy (longitudinal electrodynamic momentum); and (iv) the optical power of the initial excitation, allows us to predict the MPD of an initial beam when it reaches a thermal equilibrium.

In case of a one-band spectrum (Figs. 9a,b) the modal power distribution is always given by a Rayleigh-Jeans (RJ) law $I_\alpha = \frac{T}{\varepsilon_\alpha - \mu}$; where I_α is the power associated with the mode ε_α of the photonic network ($\alpha = 1, \cdots, N$; N is the total number of modes) and (T, μ) are the optical temperature and chemical potential (Lagrange multipliers) which are uniquely determined from the total power $\mathcal{N} = \sum_\alpha I_\alpha$ and total internal energy $\mathcal{E} = \sum_\alpha \varepsilon_\alpha I_\alpha$ of the initial beam. In Fig. 9c we demonstrate the validity of our formalism for an array of coupled nonlinear waveguides. In this example the launched beam has an initial MPD (open circles in Fig. 9c) that corresponds to (T, μ)-parameters such that the final MPD (filled black circles) follows a pre-designed RJ (red line). When the linear spectrum of the underlying photonic network exhibits bands and gaps (Figs. 9d,e), the MPD is more complex, consisting of a generalized-RJ (GRJ) distribution. This MPD describe states of a partial (or quasi) equilibrium of the system and occurred whenever the ratio between the gap-width to the band-width is larger than a critical value. The theory also predicts the relaxation times (or longitudinal propagation distances in paraxial optics) above which such non-conventional thermal states occur. Our analysis underlined the importance of band-gap engineering in the Bloch dispersion relation of a composite photonic circuit and highlighted the relaxation processes that are

responsible for the thermalization of an initial beam towards this (quasi-) stationary GRJ. Our theory has been confirmed via numerical simulations with a variety of weakly nonlinear multimode systems like the SSH model (Figs. 9d-f).

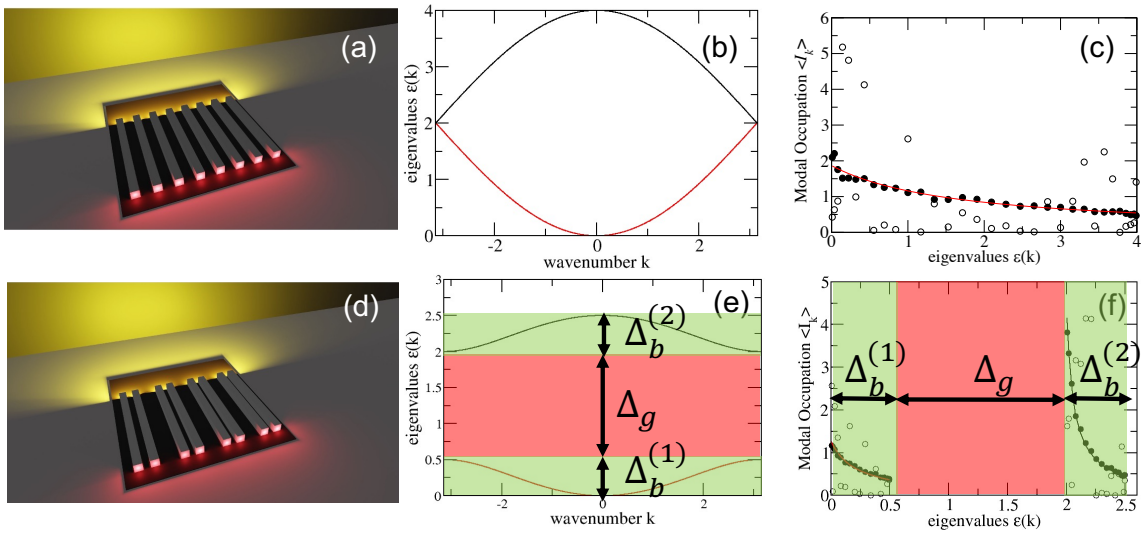

Fig. 9: *Upper row:* (a) The nonlinear multimoded photonic network consists of an array of N=32 waveguides; (b) The linear dispersion relation of this array; (c) The MPD $\langle I_k \rangle$: The initial MPD (open circles) has been designed in a way that the system will be reaching a "target" MPD which is given by a uniquely defined RJ (red line). The filled circles are the dynamical simulations of such initial beam when the latter has reached a thermal state. *Lower row*: (d) A photonic SSH circuit consisting of N=32 coupled nonlinear waveguides. The waveguides are arranged in dimers with intra-dimer coupling $v = 1$ and inter-dimer couplings $w = 1/4$ (units of v). (e) The dispersion relation of the SSH array; (f) The MPD I_k of the initial excitation (open circles) and of the thermal state (filled black circles). The solid red and black lines are the theoretical predictions describing the GRJ distribution. In both examples we have assumed a weak Kerr nonlinearity.

V. A reflective mm-wave photonic limiter: Optical limiting is a technique to protect photosensitive devices from damage caused by intense optical radiation. Optical limiters are therefore designed to block high-intensity laser radiation while transmitting low-intensity light. Most passive optical limiters utilize materials with nonlinear absorption, which are transparent to low-intensity light but turn opaque if the light intensity exceeds a certain (limiting) threshold level. A typical passive limiter, however, absorbs a significant portion of high-level radiation, which can cause overheating and damage to the limiter itself. To overcome this problem, the concept of a reflective photonic limiter (RPL), which reflects rather than absorbs high-intensity radiation, has been introduced in the past by our CDEW group. A passive reflective photonic limiter involves a photonic bandgap structure, such as a multilayer cavity, incorporating a nonlinear or a phase-change material (PCM). At low incident intensities, transmittance of the photonic structure is at its maximum due to resonant transmission via a localized mode in photonic bandgap. High-intensity radiation, however, forces nonlinearity to kick in or phase transition to be induced, producing an impedance mismatch, which reflects most of the incident radiation. The high reflectivity prevents the limiter from overheating, thereby greatly increasing the limiter damage threshold. Other important advantages of such photonic design include orders-of-magnitude larger extinction ratio (the ratio of transmittances below and above the limiting threshold) and the possibility to significantly lower the limiting threshold by adjusting the photonic structure hosting the nonlinear material or PCM.

The aforementioned approach thus provides advanced broadband protection from high-level radiation, although low-intensity transmission is essentially narrowband due to its resonant nature. Millimeter-wave limiters can be designed in much the same way to protect system receivers from high-power signals and also to allow the receivers to function normally when these high-power signals are not present.

We developed (collaboration with Prof. Chabanov/UTSA; and AFRL RY and RD) a free-

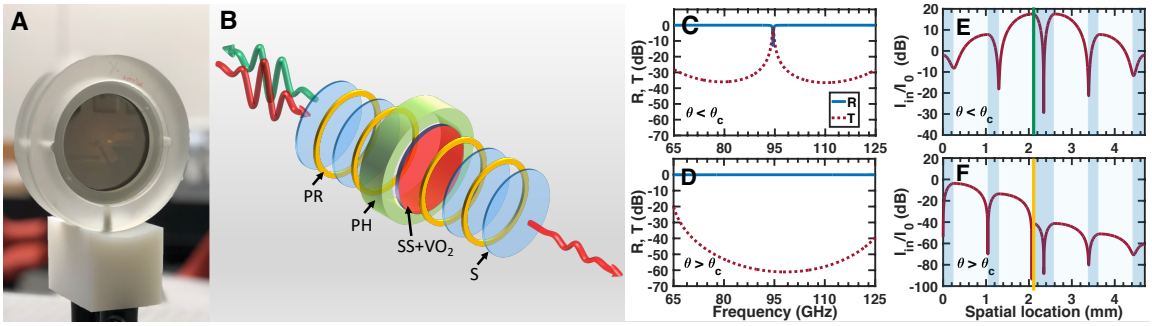

Fig. 10: A picture (**A**) and schematic (**B**) of the mm-wave photonic limiter consisting of 256-μm (S) and 525-μm (SS) thick sapphire wafers separated by 792-μm air-gap spacers (PR) and a 150-nm VO_2 layer deposited on the SS sapphire. The layer stack is retained in a plastic holder (PH). **C, D,** Simulated transmittance T and reflectance R of the photonic structure at normal incidence, at $\theta > \theta_c$ (**C**) and $\theta < \theta_c$ (**D**). **E, F,** Simulated internal intensity profiles in the direction of wave propagation of the incident intensity I_0 at the resonance frequency 95 GHz, at $\theta > \theta_c$ (**E**) and $\theta < \theta_c$ (**F**). Sapphire and air-gap layers are shown in dark and light blue, and the VO_2 layer in green and yellow at the lower and higher temperatures, respectively.

space reflective photonic limiter based on the above principles and demonstrated its implementation in the W band (95GHz). Our mm-wave limiter (see Fig. 10) is based on a resonant multilayer structure incorporating a nanolayer of vanadium dioxide (VO2), undergoing an insulator-to-metal phase transition when heated above the critical temperature of $\theta_c \approx 69$℃. The experimental results are corroborated by 3D multiphysics simulations, which allowed us to gain deeper insight into the limiting process by exploring the dynamics of the limiter driven by the VO2 phase transition. The approach based on the use of insulator-to-metal transition materials is highly scalable and can be replicated in any spectral range, from microwave (MW) to optical. With that, at MW frequencies, the insulator-to-metal transition is accompanied by much greater change in the complex permittivity of the phase-change material – orders of magnitude in our case. This provides an unprecedented flexibility in control of the MW radiation flow, unattainable in optics.

VI. A non-resonant reflective photonic limiter based on dynamical symmetries: The RPL of the previous section has the following characteristics: (a) it provides a broadband protection, (b) it demonstrates a tunable limiting threshold (LT), and (c) it exhibits a dramatically enhanced dynamical range (DR) with respect to existing limiter schemes. The concept was relying on the fact that at low incident powers the defect layer was supporting a resonant localized mode which was utilized for (near-)perfect *resonant* transmission. The physical mechanism responsible for the (near-)complete suppression of the transmission and the (near-) unity reflection was based on a self-regulated degradation of the Q-factor of the resonant mode which was triggered by the increase of the non-linear losses at the defect layer as the intensity of the incident radiation increased. The experimental implementation of such *resonant-based* RPL led to a transmittance which, for low incident powers, was approximately 50% due to Ohmic/radiative losses of the resonant modes used

in the experiment. Importantly, the previous implementations of RPLs were in-principle narrowband at low incident powers due to the resonant nature and the associated large Q-factor of the photonic-crystal resonator, which was needed to enhance the lossy nonlinearities.

During this project, we made a decisive step towards developing the concept of *non-resonant* reflective photonic limiter (NR-RPL) that exhibits (relatively-)*broadband high-transmittivity* (above 80%) for low power incident radiation without compromising the abrupt raise of reflectance to (near-)unity values at high power incident radiation. Importantly the activation time for limiting action in this new design was found from our realistic multiphysics simulations to be much shorter than the time needed for the peak of the pulse to arrive at the sample. The proposed concept of NR-RPL is based on the notion of *self-induced explicit symmetry violation of transparent modes* (TM). The TMs emerge as solutions of an auxiliary wave-operator (AWO) that is invariant under a parity-time (PT) symmetry. As opposed to typical PT-symmetric scenarios,

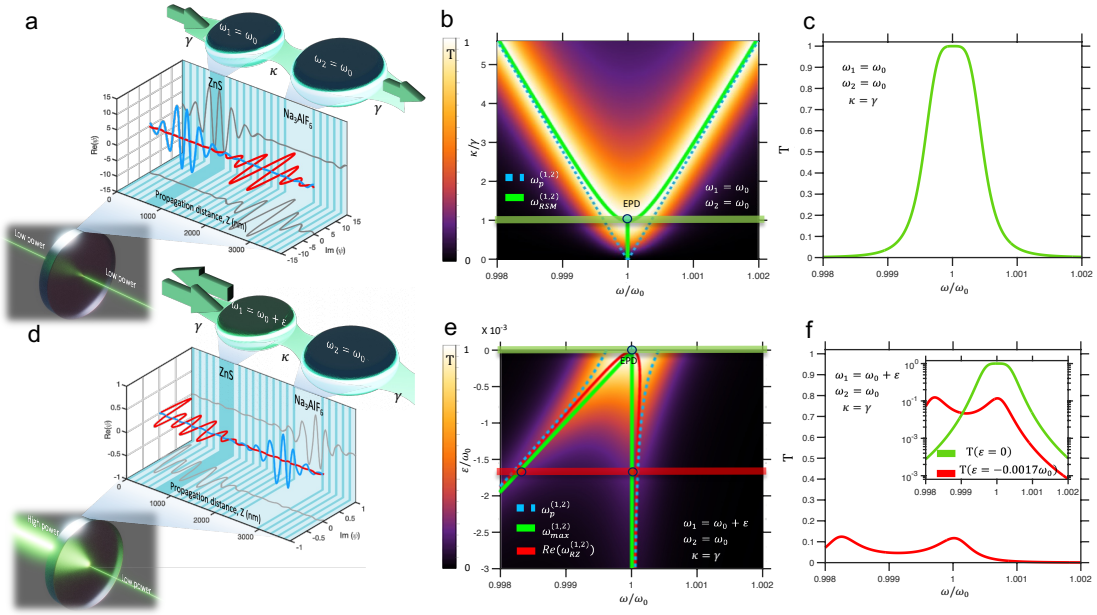

Figure 11: (a) Artistic view (bottom), schematic (middle), and CMT equivalent system (top). The CMT system consists of two coupled modes of resonance frequency $\omega_{1,2} = \omega_0$ and coupling rate κ, connected to transmission lines at coupling rates $\gamma_1 = \gamma_2 = \gamma$. It is tuned to the TM EPD by making $\kappa = \gamma$. The real and imaginary parts of the spatial field distribution for a left-incident wave of $\omega = \omega_{EPD}$ are shown in the schematic by the blue and red lines, respectively. (b) (colormap) Transmittance $T(\omega/\omega_0)$ in the parameter space of κ/γ. $T = 1$ occurs at the eigenfrequencies $\omega_{TM}^{(1,2)}$of the AWO, indicated by solid green lines. When $\kappa = \gamma$, the TMs coalesce to form an EPD-2 at $\omega_{EPD} = \omega_0$ (open circle). The horizontal green line marks the transmittance $T_{\kappa=\gamma}(\omega/\omega_0)$ plotted in (c). The dashed blue lines indicate the poles $\omega_p^{(1,2)}$ of the scattering-matrix. (c) Flat-top, near-unity transmittance $T_{\kappa=\gamma}(\omega/\omega_0)$ evaluated using CMT. (d) Same as in (a) but in the presence of the mode detuning $\omega_1 = \omega_0 + \varepsilon$. (e) (colormap) Transmittance $T_{\kappa=\gamma}(\omega/\omega_0)$ in the parameter space of ε/ω_0. The dashed blue lines indicate the eigenfrequencies $\omega_p^{(1,2)}$. The solid green lines are the trajectories of the peak transmittance frequencies $\omega_{max}^{(1,2)}$. The solid red lines indicate $\mathcal{R}e\{\omega_{TM}^{(1,2)}\}$. The horizontal red line marks the transmittance $T_{\kappa=\gamma}(\omega/\omega_0)$ for $\varepsilon/\omega_0 = -0.0017$, plotted in (f). (f) The transmittance $T_{\kappa=\gamma}(\omega/\omega_0)$ (using CMT modeling) for $\varepsilon/\omega_0 = -0.0017$. The inset shows a semi-log plot of $T_{\kappa=\gamma}(\omega/\omega_0)$ of (c) and (f).

where one requires to introduce judiciously balanced amplification and attenuation mechanisms, here the input/output channel acts as an effective "radiative gain/loss" to the system. The identification of the AWO and its hidden PT-symmetry, allowed us to "inverse-design" the NR-RPL – which, by itself, does not respect any PT-symmetry – consisting of a multilayer photonic crystal with two defect layers with the same optical length, see Figs. 11a,d. When the photonic structure is appropriately tuned, two TMs coalesce forming a second-order exceptional-point degeneracy (EPD- 2), see Fig. 11b. The latter is manifested as a flat-top, (near-)unity, transmittance line-shape in case of low power incident radiation, see Fig. 11c. On the other hand, perturbations that (spontaneously or explicitly) violate the PT-symmetry of the AWO lead to a destruction of the TMs (Figs. 11e,f) and a subsequent abrupt increase of reflectance to (near-)unity values. We have designed a family of perturbations which *explicitly* violate such PT-symmetry being related to a self-induced permittivity change (e.g. due to Kerr or thermal nonlinearities) of one defect layer when the incident radiation exceeds a critical level. In contrast to previous RPL schemes, the destruction of the TMs does not rely on nonlinear absorption mechanisms, and therefore the proposed RPL does not sustain excessive absorption at intermediate incident powers.

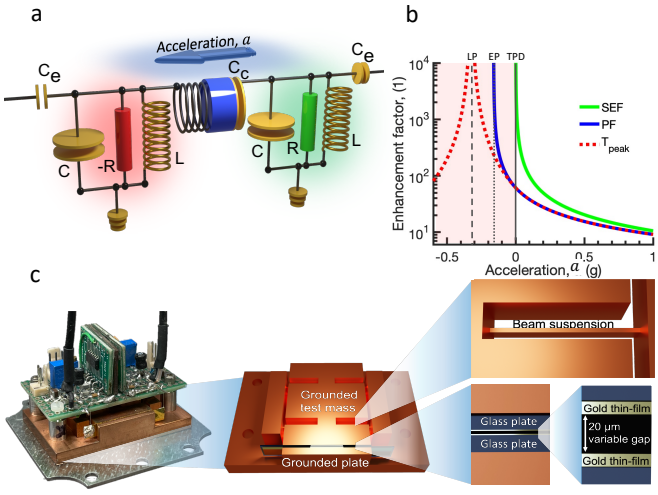

Figure 12: (a) Schematic of the $\mathcal{PT}$ -symmetric electromechanical sensor (inclinometer). The $\mathcal{PT}$-symmetric circuit is capacitively coupled to the transmission lines with a capacitor C_e. The two circuit tanks are coupled together with a variable capacitor C_c with one plate connected to a test mass that senses the acceleration. (b) The behavior of the sensitivity enhancement factor SEF (green line), Petermann factor PF which measures the bi-orthogonal nature of the eigenmodes and is responsible for the fundamental noise enhancement (blue line), and of noise enhancement factors associated with the $\mathcal{PT}$-symmetric components of the circuit $NEF^{\mathcal{PT}}$ (dark red dotted line) and the transmission line NEF^{TL} as a function of the applied acceleration a (magenta dotted line). The black vertical lines indicate the TPD (solid), EP (dotted) and LP (dashed) points. The highlighted domain indicates the accelerations which are not captured by the experimental platform. (c) The actual acceleration sensing platform utilizes a micro-fabricated coupling capacitor which is connected to the test-mass used to sense the applied acceleration/inclination.

3. Other Research Initiatives

<u>High precision inclinometers for high-energy lasers (HEL) platform stabilization:</u> Exceptional point degeneracies (EPDs) are non-Hermitian degeneracies where both eigenvalues and their corresponding eigenvectors coalesce. Recently, EPDs have attracted attention as a means to enhance the responsivity of sensors, via the abrupt resonant detuning occurring in their proximity. In many cases, however, the EPD implementation is accompanied by noise enhancement leading to the degradation of sensor's performance. The excess noise can be of fundamental nature (due to the eigenbasis collapse) or of technical nature associated with the amplification mechanisms utilized for the realization of EPDs. In a recent publication, we have shown using an EPD-based $\mathcal{PT}$-symmetric electromechanical accelerometer/ inclinometer (see Fig. 12), that the enhanced technical noise can be surpassed by the enhanced responsivity to applied accelerations. The noise due to eigenbasis collapse

is mitigated by exploiting the detuning from a transmission peak degeneracy (TPD) – which forms when the sensor is weakly coupled to transmission lines – as a sensitivity measurant. These TPDs occur at a frequency and controlled parameters for which the bi-orthogonal eigen-basis is still complete and are distinct from the EPs of the $\mathcal{PT}$-sensor. Our device demonstrated a three-fold signal-to-noise ratio enhancement compared to configurations for which the system operates away from the TPD.

In parallel to the above activity, we proposed a passive non-resonant (NR) EPD-sensor that is resilient to losses, local cavity variations and noise. The NR-EPD describes the coalescence of Bloch eigenmodes associated with the spectrum of transfer matrices of periodic structures. This coalescence enables scattering cross-section cusps with a sublinear response to small detunings away from an NR-EPD. We show that these cusps can be utilized for enhanced noise-resilient sensing.

4. Training Opportunities

During this period, one graduate student has awarded his degree (Dr. Suwun Suwunnarat—PhD). Dr. Suwunnarat is currently a lecturer at KOSEN-KMITL. The post-doctoral associate Dr. Rodion Kononchuk has moved to Silicon Valley where he works as an R&D researcher for MEMS development with A. M. Fitzgeral & Associates, LLC. Finally, the post-doctoral associate Dr. Lucas Fernandez-Alcazar is now Assistant Researcher at CONICET with a joint appointment as Assistant Professor of Physics at University of Corrientes-Argentina. Four undergraduate students that have been involved in this research activity have been accepted to high-profile graduate programs in physics, applied mathematics or electrical engineering (Princeton, Columbia, USC, etc.).

The PI and senior members of the CDEW research team have offered a number of individual research tutorials during the period of this grant. As a result of these tutorials, the Wesleyan team has attracted during each summer a number of undergraduate students that eventually joint the group working on research related to our project. One of these undergraduate students has been admitted to the Wesleyan competitive BA/MA program and is doing his Master research work with the CDEW team. The PI has been also involved in outreach programs and has given lectures on optics and photonics to K12 students (raising juniors) at local high-schools. Finally, the PI was invited to give two hours Zoom lecture on anti-linear symmetries and their applications in photonics at the META doctoral school, organized in New York in September 2021.

5. Dissemination of Results

The results of this effort have been disseminated to various forums: conferences, DOD lab seminars, and department colloquia [twenty events in total]. During the period of the grant we have published fifteen peer reviewed papers which were partially or fully supported by this effort.

All our results became eventually available on on-line professional databases like the ArXiv. We were also invited and presented invited talks on our results in professional meetings and university colloquia (see Sec. 9 for a detail list of presentations). The group manages the Theory seminar at the Physics Department of Wesleyan University which is appropriate for general student audience. The goal is to recruit and attract students in photonics. The group is committed to dissemination of knowledge to general public. In this spirit, the PI also gave a first-year-seminar for freshmen at Wesleyan University. As a result, we were able to recruit one freshman who is currently working with the Wesleyan team, on a theme related to the current proposal.

The group has strong contacts with DoD Labs (AFRL at Wright-Patterson) where we regularly disseminate our results either via email correspondence or via presentations/talks. For example, Dr. I. Vitebskiy AFRL/RY has recently visited Wesleyan University to collaborate with us on the analysis of beam propagation in systems with frozen mode and nonlinearities. It is envisioned that such photonic structures can be used for high-power lasers and/or low-noise amplifiers. We have also participated in AFRL working meetings with academia that aimed to discussed wave transport in photonic structures that support a frozen mode regime.

6. Technology Transfer and Impact

The group has filed for two patents:

a) US Patent App. 17/550915, Systems, methods, and media for wireless power transfer, Lei Chen, Steven Mark Anlage, Tsampikos Kottos, 14/12/2021, approved.
b) US Patent App. 17/681320, Electromechanical Force Sensor Based on Extrema Degeneracy Point with Nonlinear Response, R. Thevamaran, J. Cai, T. Kottos, F. Ellis, R. Kononchuk, 02/25/2022, Pending.

We have also transition designs of reflective photonic limiters with phase-change materials at W-band to the Directed Energy Directorate of the AFRL-Kirtland (B. Hoff) and to the AFRL-Wright-Patterson RY (I. Vitebskiy). Along these lines we have performed the modeling and the analysis and interpretation of experimental data taken at Kirtland.

Recently, we have transitioned a new concept of non-resonant reflective photonic limiters based on dynamical symmetries to the AFRL.

7. Collaborations

The Wesleyan group has developed a strong collaboration with two AFRL groups – one at AFRL/RY Wright Patterson [Dr. I. Vitebskiy; RY] and another one at AFRL/RD Kirckland [Dr. Brad Hoff; RD]. Our role in this collaboration was to provide a theoretical support and design of reflective photonic limiters. In parallel, we have developed collaboration on wavefront shaping schemes with the experimental groups of Prof. S. Anlage from UMD, and Profs. U. Kuhl and F. Mortessagne from CNRS/ Universite Cote d' Azur, Institute de Physique. We also developed a collaboration with Prof. B. Shapiro (Technion/ Israel) on statistical description of thermal states in multimoded nonlinear photonic networks. Outcomes of these collaborations have been documented via publications in peer reviewed journals [see publications, Sec. 9].

8. Wesleyan University Team members

PI: Dr. Tsampikos Kottos.
Post-doctoral associates: Lucas Fernandez-Alcazar; Rodion Kononchuk; Arkady Kurnosov; Mona Nafari; Alba Ramos; Chengzhen Wang.
Graduate students: Zhi-Ming Gan; John Guillamon; Suwun Suwunnarat; William Tuxbury.
Undergraduate students: Abe Bradley; Ted Heitzmann; Do-Hyeok Jeon; Serenal Landers; Joe Pollack; Ben Reilly; Cheng Shi; Yaqian Tang.

8. Honors/Awards Received During the Period of the Grant

1) Dr. Tsampikos Kottos (PI) has been appointed the "Lauren B. Dachs" endowed Professor of Science and Society, July 2019.
2) Dr. Tsampikos Kottos (PI) has been awarded the 2019 Wesleyan Faculty Award for Excellence in Research, September 2019.
3) Dr. Tsampikos Kottos (PI) was appointed member of the Steering Committee of the Simons Collaboration Project in *MPS "Harnessing Universal Symmetry Concepts for Extreme Wave Phenomena"*
4) Do Hyeok Jeon (undergraduate student), Phi-Beta-Kappa, December 2020
5) Cheng Shi (undergraduate student), Phi-Beta-Kappa, June 2022
6) Do Hyeok Jeon (undergrad student), Carl Van Dyke Prize[1], Wesleyan Univ., May 2020
7) Cheng Shi (undergrad student), Carl Van Dyke Prize[1], Wesleyan Univ., May 2021 & May 2022
8) Ben Reilly (undergrad student), Carl Van Dyke Prize[1], Wesleyan Univ., May 2021

9. Publications, Patents, Thesis, Lectures/Talks etc

Publications

1) Rodion Kononchuk, Suwun Suwunnarat, Martin S. Hilario, Anthony E. Baros, Brad W. Hoff, Vladimir Vasilyev, Ilya Vitebskiy, Tsampikos Kottos, Andrey A. Chabanov, *A reflective millimeter-wave photonic limiter,* Science Advances 8, eabh1827 (2022).
2) William Tuxbury, Rodion Kononchuk, Tsampikos Kottos, *Non-resonant exceptional points as enablers of noise-resilient sensors,* Communications Physics 5, 210 (2022).
3) Suwun Suwunnarat, Taqian Tang, Mattis reisner, Fabrice Mortessagne, Ulrich Kuhl, Tsampikos Kottos, *Non-linear coherent perfect absorption in the proximity of exceptional points*, Communications Physics 5, 5 (2022)
4) Abe Bradley, William Tuxbury, Tsampikos Kottos, *Directed emission from uniformly excited non-Hermitian structures,* Opt. Lett. 47, 5913 (2022).
5) R. Kononchuk, J. Cai, Fred Ellis, Ramathasan Thevamaran, Tsampikos Kottos, *Exceptional-point-based accelerometers with enhanced signal-to-noise ratio,* Nature 607, 697 (2022)
6) Cheng Shi, Tsampikos Kottos, Boris Shapiro, *Controlling optical beam thermalization via band-gap engineering*, Phys. Rev. Research 3, 033219 (2021).
7) W. Tuxbury, L. J. Fernandez-Alcazar, I. Vitebskiy, T. Kottos, *Scaling theory of absorption in the frozen mode regime*, Opt. Lett. 46, 3053 (2021).
8) Lucas J. Fernandez-Alcazar, Rodion Kononchuk, Tsampikos Kottos, *Enhanced energy harvesting near exceptional points in systems with (pseudo)-PT-symmetry*, Comm. Phys. 4, 79 (2021).
9) Alba Ramos, Lucas Fernandez-Alcazar, Tsampikos Kottos, Boris Shapiro, *Optical Phase Transitions in Photonic Networks: a Spin-System Formulation*, Phys. Rev. X 10, 031024 (2020)

---

[1]The Carl Van Dyke award is given by the Physics Department of Wesleyan University "to students majoring in physical science who show outstanding academic achievement and a promise of productivity in a professional career"

10) Rodion Kononchuk, Tsampikos Kottos, *Orientation-sensed optomechanical accelerometers based on exceptional points*, Phys. Rev. Research 2, 023252 (2020)
11) Q. Zhong, L. Simonson, T. Kottos, R. El-Ganainy, *Coherent virtual absorption of light in microring resonators*, Phys. Rev. Research 2, 013362 (2020).
12) Do Hyeok Jeon, Mattis Reisner, Fabrice Mortessagne, Tsampikos Kottos, Ulrich Kuhl, *Non-Hermitian CT-Symmetric Spectral Protection of Nonlinear Defect Modes*, Phys. Rev. Lett. 125, 113901 (2020)
13) Suwun Suwunnarat, Rodion Kononchuk, Andrey Chabanov, Ilya Vitebskiy, Nicholaos Limberopoulos, Tsampikos Kottos, *Enhanced nonlinear instabilities in photonic circuits with exceptional point degeneracies*, Photonics Research 8, 737 (2020).
14) Lei Chen, Tsampikos Kottos, Steven Anlage, *Perfect absorption in complex scattering systems with or without hidden symmetries*, Nature Communications 11, 5826 (2020)
15) M. Reisner, F. Mortessagne, E. Makri, T. Kottos, U. Kuhl, *Microwave Limiters Implemented by Coupled Dielectric Resonators Based on a Topological Defect Mode and CT-Symmetry Breaking*, APPA 136, 790 (2019).

Papers submitted for publication

1) C-Z. Wang, R. K*ononchu*k, U. Kuhl, T. Kottos, *Universalities of Asymmetric Transport in Nonlinear Wave Chaotic Systems*, submitted (2022)
2) A. Y. Ramos, C. Shi, L. J. Fernandez-Alcazar, D. N. Christodoulides, T. Kottos, *Disorder-hindered optical thermalization in nonlinear multimoded photonic circuits*, submitted (2022).

Patents

1) US Patent App. 17/550915, Systems, methods, and media for wireless power transfer, Lei Chen, Steven Mark Anlage, Tsampikos Kottos, 14/12/2021, Accepted.
2) US Patent App. 17/681320, Electromechanical Force Sensor Based on Extrema Degeneracy Point with Nonlinear Response, R. Thevamaran, J. Cai, T. Kottos, F. Ellis, R. Kononchuk, 02/25/2022, Pending

Theses

Suwun Suwunnarat, *Wavefront Shaping Protocols for Targeted Energy Deposition and Limiter Protection*, Wesleyan University (12/30/2021)

Invited Talks in Conferences/Worlshops/Colloquia

1) T. Kottos, Optical beam thermalization in non-linear multimode fibers, Invited Talk, International Conference on Laser Filamentation (COFIL) 2022, 11-15 July 2022, Chania, Greece.
2) T. Kottos, Optical beam thermalization in non-linear multimoded fibers, Invited Talk, The 12th IMACS International Conference on Nonlinear Evolution Equations and Wave Phenomena: Computation and Theory, 03/30/22-04/01/22, Athens, Georgia, USA.
3) T. Kottos, Wave-Matter interactions in the proximity of Non-Hermitian singularities, XVII Brunel-Bielefeld Workshop on RMT and Applications, Bielefeld-Germany, December 16-18 (2021).
4) T. Kottos, Exceptional Point Degeneracies in Micro-mechanical Structures: Theoretical Challenges and Technological Applications, Invited Talk, Metamaterials Conference, New York, September 20-25 (2021).

5) T. Kottos, Exceptional Points and PT -Symmetric Structures, Invited Lecturer, META Doctoral School, New York, September 24-25 (2021).
6) T. Kottos, Reflective Receiver Protectors with non-Hermitian CT-symmetric Spectral protection of Nonlinear Defect Modes, Invited Talk, SPIE Optics+Photonics, 1-5 August (2021).
7) T. Kottos, Optical phase transitions in photonic networks: a spin system formulation, GdR Cocmplexe Annual Workshop (Online), November 30-December 2 (2020)
8) T. Kottos, *Optical phase transitions in photonic networks: a spin system formulation*, Metamaterials2020, New York, October 1st (2020).
9) T. Kottos, *Robust Scattered Fields from Adiabatically Driven Targets around Exceptional Points*, Metamaterials2020, New York, September 29th (2020).
10) T. Kottos, *Reflective Limiters based on EP Degeneracies,* Annual Directed Energy Science & Technology Symposium, Invited Talk, West Point NY, March 9-13 (2020)
11) T. Kottos, *Light propagation in disordered multimode fibers, Control of Quantum and Classical Waves in Complex Media*, Invited Talk, Ein-Gedi Israel, February 19 (2020)
12) T. Kottos, *Time-Reversal Symmetty and its Applications: From Waveform Shaping to System Protection*, VII Leopoldo Garcia-Colin Mexican meeting on Mathematical and Experimental Physics, Plenary Lecture, Mexico City, February 17 (2020)
13) Suwun Suwunnarat, *Reflective Limiters based on Exceptional Point Degeneracies*, Metamaterials2020, New York, September 29th (2020)
14) Rodion Kononchuk, *Accelerometers based on Exceptional Points*, Metamaterials2020, New York, September 29th (2020)
15) T. Kottos, *Light propagation in disordered multimode fibers, Control of Quantum and Classical Waves in Complex Media*, Invited Talk, Ein-Gedi Israel, February 19 (2020)
16) T. Kottos, *Time-Reversal Symmetty and its Applications: From Waveform Shaping to System Protection*, VII Leopoldo Garcia-Colin Mexican meeting on Mathematical and Experimental Physics, Plenary Lecture, Mexico City, February 17 (2020)
17) T. Kottos, *Light Propagation in Disordered Multimode Fibers*, Invited Talk to US-Middle-East Conference on Photonics, New York, November 4-6 (2019)
18) T. Kottos, *A quest for Extreme Wave-Matter Interactions and the Emergence of New Technologies*, Key Note Lecture, Summer Research Program, Wesleyan Univ., July 25 (2019).
19) Do Hyeok Jeon, *Self-shielded receiver protectors using topological photonic circuits*, Foundations of Nonlinear Optics 2019, Contributed Talk, Air Force Institute of Technology, August 6-8 (2019).
20) Lucas Fernandez, *Chiral control of the scattering field by quasi-static encircling of an exceptional point*, Contributed Talk, US-Middle East Conference on Photonics: Early Career Symposium, New York, November 4-6 (2019).

10. Point of Contact in Navy

Mr. Peter A. Morrison, Office of Naval Research
Email: peter.a.morrison@navy.mil

REPORT DOCUMENTATION PAGE

1. REPORT DATE	2. REPORT TYPE	3. DATES COVERED	
		START DATE	END DATE
11/28/2022	Final Technical Report	07/01/2019	10/31/2022

4. TITLE AND SUBTITLE

The Wesleyan University Research Effort for: Waveform Shaping Protocols for Targeted Electromagnetic Attacks

5a. CONTRACT NUMBER	5b. GRANT NUMBER	5c. PROGRAM ELEMENT NUMBER
	N00014-19-1-2480	

5d. PROJECT NUMBER	5e. TASK NUMBER	5f. WORK UNIT NUMBER

6. AUTHOR(S)

Kottos, Tsampikos

7. PERFORMING ORGANIZATION NAME(S) AND ADDRESS(ES)	8. PERFORMING ORGANIZATION REPORT NUMBER
Wesleyan University 237 High Street Middletown CT, 06459-3208	3YVU6

9. SPONSORING/MONITORING AGENCY NAME(S) AND ADDRESS(ES)	10. SPONSOR/MONITOR'S ACRONYM(S)	11. SPONSOR/MONITOR'S REPORT NUMBER(S)
ONR REG Office Boston 495 Summer Street, Room 627 BOSTON MA 02210-2109	ONR	N62879

12. DISTRIBUTION/AVAILABILITY STATEMENT

Approved for Public Release; Distribution is Unlimited

13. SUPPLEMENTARY NOTES

14. ABSTRACT

The objective of this project is to exploit new concepts and develop theoretical/computational schemes (and demonstrate their efficiency) for the design of Wavefronts with Enhanced TArgeting Capabilities (WETAC) of linear and nonlinear electronic targets that are located inside complicated enclosures. On the counter-side, the effort also develops novel protection schemes against agile wavefronts that aim to damage sensitive US assets (e.g., radars)

15. SUBJECT TERMS

wavefront shaping, coherent perfect absorbers, statistical theory of electromagnetic transport, nonlinear wave transport, chaos, reflective photonic limiters, sensors

16. SECURITY CLASSIFICATION OF:			17. LIMITATION OF ABSTRACT	18. NUMBER OF PAGES
a. REPORT	b. ABSTRACT	C. THIS PAGE		
U	U	U	UU	

19a. NAME OF RESPONSIBLE PERSON	19b. PHONE NUMBER *(Include area code)*
Tsampikos Kottos	860-685-2036

PREVIOUS EDITION IS OBSOLETE.

STANDARD FORM 298 (REV. 5/2020)

Prescribed by ANSI Std. Z39.18